Computational Analysis of the Potential Energy Surfaces of Glycerol in the Gas and Aqueous Phases: Effects of Level of Theory, Basis Set, and Solvation on Strongly Intramolecularly Hydrogen-Bonded Systems

Christopher S. Callam, Sherwin J. Singer, Todd L. Lowary,* and Christopher M. Hadad*

Contribution from the Department of Chemistry, The Ohio State University, 100 West 18th Avenue, Columbus, Ohio 43210

Received July 23, 2001. Revised Manuscript Received September 10, 2001

Abstract: The 126 possible conformations of 1,2,3-propanetriol (glycerol) have been studied by ab initio molecular orbital and density functional theory calculations in the gas and aqueous phases at multiple levels of theory and basis sets. The partial potential energy surface for glycerol as well as an analysis of the conformational properties and hydrogen-bonding trends in both phases have been obtained. In the gas phase at the G2(MP2) and CBS-QB3 levels of theory, the important, low-energy conformers are structures **100** and **95**. In the aqueous phase at the SM5.42/HF/6-31G* level of theory, the lowest energy conformers are structures **95** and **46**. Boltzmann distributions have been determined from these high-level calculations, and good agreement is observed when these distributions are compared to the available experimental data. These calculations indicate that the enthalpic and entropic contributions to the Gibbs free energy are important for an accurate determination of the conformational and energetic preferences of glycerol. Different levels of theory and basis sets were used in order to understand the effects of nonbonded interactions (i.e., intramolecular hydrogen bonding). The efficiency of basis set and level of theory in dealing with the issue of intramolecular hydrogen bonding and reproducing the correct energetic and geometrical trends is discussed, especially with relevance to practical computational methods for larger polyhydroxylated compounds, such as oligosaccharides.

I. Introduction

Polyhydroxylated molecules such as carbohydrates play an important role in biology. In particular, oligosaccharides have been implicated in a host of important biological processes ranging from fertilization to bacterial and viral infection to the metastasis of cancer.[1] The structure and conformation of an oligosaccharide are critical to its function, and there has been increasing interest in understanding the conformation of these molecules.[2] Oligosaccharides are, in general, flexible species that often exist in solution as an ensemble of conformers. Accordingly, the use of computational chemisty is almost always required in conjunction with NMR spectroscopic experiments in order to understand the solution conformation of these molecules.[2,3] To adequately address the conformational flexibility of these systems using ab initio and density functional theory (DFT) methods, one needs not only to use high levels of theory and good basis sets but also to consider a variety of conformations and the effect of solvation.

With carbohydrates as well as other polyhydroxylated compounds, the use of gas-phase computational methods leads to optimized conformers possessing many intramolecular hydrogen bonds. An important issue that must be considered is how relevant the calculated gas-phase structures are compared to those found in an aqueous environment.[4] In water, it may be expected that intramolecular hydrogen bonding will be minimized through interaction of the carbohydrate with the solvent. In furanose rings, the issue of intramolecular hydrogen bonding is particularly important. Given the inherent flexibility of five-membered rings, the formation of one or two strong intramolecular hydrogen bonds can often significantly stabilize some ring conformers relative to others. This, in turn, can lead to the possibility of discrepancies when compared to experiment. For example, in our own ab initio and DFT investigations of the arabinofuranose ring,[5−9] we have found that, in some cases, good agreement with experimental results is observed,[6,9] while, in others, the agreement is poorer.[5,7] In one case,[5] we attempted, unsuccessfully, to improve correlation between computed and experimental results by optimizing geometries that were prohibited from forming intramolecular hydrogen bonds. This

(1) Recent reviews: (a) Varki, A. *Essent. Glycobiol.* **1999**, 57. (b) Dwek, R. A. *Chem. Rev.* **1996**, *96*, 683.

(2) Recent reviews: (a) Homans, S. W. *Carbohydr. Chem. Biol.* **2000**, *2*, 947. (b) Imberty, A.; Perez, S. *Chem. Rev.* **2000**, *100*, 4567.

(3) Recent reviews: (a) Bush, C. A.; Martin-Pastor, M.; Imberty, A. *Annu. Rev. Biophys. Biomol. Struct.* **1999**, *28*, 269. (b) Poveda, A.; Asensio, J. L.; Espinosa, J. F.; Martin-Pastor, M.; Canada, J.; Jimenez-Barbero, J. *J. Mol. Graphics. Modell.* **1997**, *15*, 9.

(4) (a) Cramer, C. J.; Truhlar, D. G. *J. Am. Chem. Soc.* **1993**, *115*, 5745. (b) Kollman, P. A. In *Modern Theoretical Chemisty*; Schaefer, H. F., III, Ed.; Plenum: New York, 1977; Vol. 4, Chapter 3. (c) Hobza, P.; Zahradnik, R. *Chem. Rev.* **1988**, *88*, 871. (d) Kumpf, R. A.; Damewood, J. R., Jr. *J. Phys. Chem.* **1989**, *93*, 4478.

(5) Gordon, M. T.; Lowary, T. L.; Hadad, C. M. *J. Am. Chem. Soc.* **1999**, *121*, 9682.

(6) Gordon, M. T.; Lowary, T. L.; Hadad, C. M. *J. Org. Chem.* **2000**, *65*, 4954.

(7) McCarren, P. R.; Gordon, M. T.; Lowary, T. L.; Hadad, C. M. *J. Phys. Chem. A* **2001**, *105*, 5911.

(8) Houseknecht, J. B.; McCarren, P. R.; Lowary, T. L.; Hadad, C. M. *J. Am. Chem. Soc.* **2001**, *123*, 8811.

(9) McCarren, P. R.; Lowary, T. L.; Hadad, C. M. Manuscript in preparation.

10.1021/ja011785r CCC: $20.00
Published on Web 10/31/2001

Chart 1

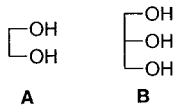

underscores the importance of explicitly considering solvation in these calculations, and in another study,[8] we have found that closer agreement with experiment is observed when the geometry optimizations are carried out using the MN-GSM[10] solvation model.

We have been prohibited from considering all possible conformations of the carbohydrate systems of interest to us because of their size. However, we viewed it important to exhaustively investigate all conformers of at least one flexible molecule that was capable of forming a number of intramolecular hydrogen bonds. In an earlier study, Cramer and Truhlar used 1,2-ethanediol (ethylene glycol, **A**, Chart 1) for this purpose.[11a] In their investigation, the relative energies of all 20 unique conformers of **A** were optimized in both the gas phase and in aqueous solution with the AMSOL model. Using this approach, it was discovered that the percentage of intramolecularly hydrogen-bonded conformers was only slightly smaller in solution than in the gas phase. 1,2-Ethanediol is capable of forming only five-membered ring intramolecular hydrogen bonds. In carbohydrates, however, the formation of five-, six-, and, in some cases, seven-membered ring hydrogen bonds is possible, and thus, the situation is more complex than that for **A**. Accordingly, we view 1,2,3-propanetriol (glycerol, **B,** Chart 1) as an ideal model system for studying intramolecular hydrogen bonds in carbohydrates, as the presence of three hydroxyl groups gives rise to particularly complex and diverse conformational possibilities, including both five- and six-membered ring hydrogen bonds.

The conformation of glycerol has been extensively studied in the gas,[12] liquid,[13] and solid states,[14] and the conformational space of the molecule is quite complex. Although glycerol contains no asymmetric carbons, conformational isomerism renders it prochiral. There are six backbone conformations that are designated by the dihedral angles involving the carbon and oxygen atoms ($\alpha\alpha$, $\alpha\beta$, $\alpha\gamma$, $\beta\beta$, $\beta\gamma$, and $\gamma\gamma$, see later).[12a] However, these six backbone conformations are not correlated with the orientations of the hydroxyl groups.

All of the conformational isomers differ by specification of the five possible dihedral angles: one about each of the two C−C bonds and three about each C−O bond. Assuming typical staggered conformational energy profiles for these bonds, with minima for dihedral angles near 60°, 180°, and 300°, this gives rise to 486 possible conformational isomers. This number can be obtained by fixing bonds 1 and 2 (Figure 1) in a coordinate system and allowing bonds 3−8 to have all of the possible staggered orientations. There are 3 possibilities for bonds 3−6 and 8, but bond 7 (once bond 4 is fixed) can only take two values. Therefore, the number of primitive conformations is $2 \times (3^5)$. After the 486 configurations are generated, symmetric-redundant conformers can be eliminated, thereby reducing the total to 126. Of these, 117 conformers are 4-fold degenerate, and 9 conformers are 2-fold degenerate. (All 126 unique staggered conformations are listed in the Supporting Information along with the degeneracy of each.)

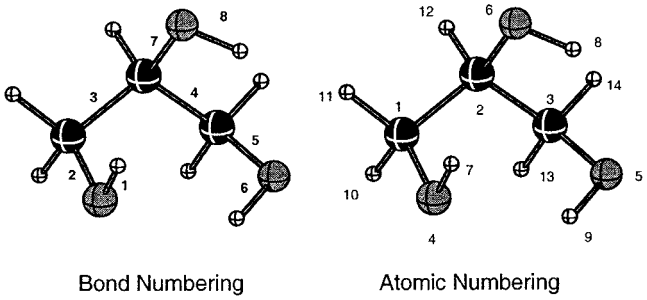

Figure 1. Bond numbering and atomic numbering used for glycerol conformations.

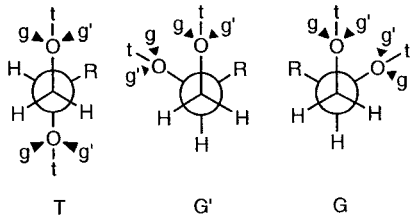

Figure 2. Conventional nomenclature system for the dihedral angles (g, t, g′) and C−C torsion angles (G, T, G′).

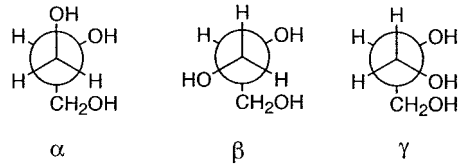

Figure 3. Backbone conformations and their nomenclature system.

Following the conventional notation, the dihedral angles noted above are designated g, t, and g′, respectively, for gauche clockwise, trans, and gauche counterclockwise for the C−O torsion, and also G, T, and G′ for the analogous C−C torsion angles (Figure 2).[15] Symmetry in the form of an internal mirror plane bisecting the central C−O bond relates isomers via an internal reflection process. Conformational isomers without the presence of any symmetry elements possess enantiomeric conformations. For example, using the definitions described above, one finds that gTg′,gGg′ is the enantiomer of g′Gg,g′Tg. For each conformer discussed below, a unique number was assigned on the basis of the algorithm used to generate the structure. The backbone conformations have also been assigned to each of the structures according to the previously described nomenclature system by Bastiansen[12a] which takes into account only the two O−C−C−C torsion angles. Each CH_2OH group can rotate around a C−C bond, giving rise to the α, β, and γ conformations.[12a] Figure 3 illustrates the respective orientations of the oxygen atoms with respect to the possible backbone conformations. This gives rise to six possible backbone con-

(10) (a) Xidos, J. D.; Li, J.; Hawkins, G. D.; Liotard, D. A.; Cramer, C. J.; Truhlar, D. G.; Frisch, M. J. *MN-GSM*, version 99.2; University of Minnesota: Minneapolis, MN. (b) Li, J. B.; Zhu, T. H.; Cramer, C. J.; Truhlar, D. G. *J. Phys. Chem. A.* **1998**, *102*, 1820. (c) Li, J. B.; Hawkins, G. D.; Cramer, C. J.; Truhlar, D. G. *Chem. Phys. Lett.* **1998**, *288*, 293. (d) Zhu, T. H.; Li, J. B.; Hawkins, G. D.; Cramer, C. J.; Truhlar, D. G. *J. Chem. Phys.* **1998**, *109*, 9117. (e) Li, J. B.; Zhu, T.; Hawkins, G. D.; Winget, P.; Liotard, D. A.; Cramer, C. J.; Truhlar, D. G. *Theor. Chem. Acc.* **1999**, *103*, 9.

(11) (a) Cramer, C. J.; Truhlar, D. G. *J. Am. Chem. Soc.* **1994**, *116*, 3892. (b) For other studies of ethylene glycol, see: Bultinck, P.; Goeminne, A.; Van de Vondel, D. *THEOCHEM* **1995**, *357*, 19 and references therein.

(12) (a) Bastiansen, O. *Acta Chem. Scand.* **1949**, *3*, 415. (b) Maccaferri, G.; Caminati, W.; Favero, P. G. *J. Chem. Soc., Faraday Trans.* **1997**, *93*, 4115.

(13) (a) Champeney, D. C.; Joarder, R. N.; Dore, J. C. *Mol. Phys.* **1986**, *58*, 337. (b) Garawi, M.; Dore, J. C.; Champeney, D. C. *Mol. Phys.* **1987**, *62*, 475.

(14) Dawidowski, J.; Bermejo, F. J.; Fayos, R.; Perea, R. F.; Bennington, S. M.; Criado, A. *Phys. Rev. E* **1996**, *53*, 5079.

(15) Radom, L.; Lanthan, W. A.; Hehre, W. J.; Pople, J. A. *J. Am. Chem. Soc.* **1973**, *95*, 693.

Table 1. Relative Energies of Gas-Phase Conformers Calculated from HF/6-31G* Geometries for the Lowest 35 Conformers[a]

conformer number	backbone	conformer	HF/6-31G*	B3LYP/6-31+G**//HF/6-31G*	B3LYP/6-311+G(3df,2p)//HF/6-31G*	G2(MP2)	CCSD/6-31+G**//HF/6-31G*	CCSD(T)/6-31+G**//HF/6-31G*
95	$\alpha\gamma$	tG′g,tG′g	0.00	0.00	0.00	0.21	0.00	0.02
100	$\gamma\gamma$	gG′g,g′Gg	0.27	0.22	0.15	0.00	0.27	0.00
109	$\alpha\alpha$	gG′t,g′Gt	0.80	0.38	0.27	0.79	0.75	0.82
46	$\alpha\gamma$	gGg′,tGg′	0.74	0.54	0.30	0.61	0.73	0.65
101	$\gamma\gamma$	tG′g,g′Gg	1.04	0.78	0.72	0.64	0.86	0.70
7	$\alpha\alpha$	gGg′,tG′g	1.40	0.80	0.48	1.09	1.29	1.27
48	$\alpha\gamma$	g′Gg,g′Gt	1.33	1.05	0.81	1.06	1.26	1.24
120	$\alpha\alpha$	gG′g,tGg′	1.94	1.33	0.86	1.54	1.65	1.64
45	$\gamma\alpha$	g′Gg,tGg′	1.58	1.40	1.08	1.50	1.51	1.46
43	$\gamma\alpha$	gGg′,gGg′	2.27	1.70	1.18	1.52	2.13	2.00
20[b]	$\alpha\beta$	tGg′,tTt	1.85	1.98	1.61	2.12	2.08	2.29
2	$\alpha\beta$	tGg′,tTg	1.97	2.05	1.55	2.17	2.27	2.41
116	$\alpha\beta$	g′G′g,tTt	2.12	2.06	1.57	2.15	2.29	2.51
9	$\alpha\alpha$	g′Gg,g′G′g	3.09	2.19	1.43	2.17	2.99	2.87
34	$\gamma\beta$	tGg′,gTt	2.14	2.23	1.74	2.62	2.88	2.66
1	$\alpha\beta$	gGg′,tTg′	2.60	2.44	1.75	2.45	2.81	2.85
64	$\beta\gamma$	tTg,g′Gg	2.31	2.47	1.90	2.08	2.24	2.25
86	$\beta\alpha$	tTg,tGg′	2.55	2.48	1.92	2.58	2.61	2.20
54	$\beta\gamma$	g′Tg,tG′g	2.13	2.51	1.91	2.24	2.25	2.25
80	$\beta\gamma$	gTg,g′Gt	2.51	2.58	1.94	2.27	2.72	2.76
53	$\beta\gamma$	tTg,tG′g	2.39	2.58	1.96	2.30	2.55	2.63
66	$\beta\gamma$	gTg,g′Gg	2.48	2.63	1.92	2.34	2.65	2.61
85	$\beta\alpha$	gTg,tGg′	2.93	2.78	2.06	2.80	2.76	2.58
18	$\gamma\beta$	g′Gg,tTg	2.44	2.85	2.20	2.37	2.47	2.44
75	$\beta\beta$	g′Tg,tTt	2.55	2.85	2.40	2.88	3.01	3.08
78	$\beta\gamma$	gTg,g′Gt	2.65	2.85	2.22	2.44	2.61	2.63
35	$\gamma\beta$	g′Gg,tTt	2.78	2.94	2.24	2.62		
103	$\alpha\beta$	gG′t,g′Tg	3.24	3.05	2.27	3.02		
88	$\beta\beta$	g′Tg,tTg′	2.76	3.07	2.49	3.10		
106	$\alpha\gamma$	tG′g,tG′t	3.60	3.11	2.41	3.00		
105[b]	$\alpha\beta$	g′G′g,tTg	3.33	3.14	2.25	2.97		
104	$\alpha\beta$	tG′g,tTg	3.18	3.14	2.35	3.03		
114	$\alpha\beta$	gG′g,tTt	3.21	3.27	2.44	2.38		
21	$\alpha\beta$	g′Gg,g′Tt	3.85	3.40	2.51	3.24		
3	$\alpha\beta$	g′Gg,g′Tg	3.83	3.42	2.48	3.30		
av difference from G2(MP2) (kcal/mol) (75)[c]			0.59	0.35	0.65			
av difference from G2(MP2) (kcal/mol) (25)[c]			0.25	0.20	0.45		0.21	0.21
av difference from G2(MP2) (kcal/mol) (12)[c]			0.26	0.17	0.41		0.19	0.14
slope vs G2(MP2) (75)[c]			0.81	0.86	1.07			
slope vs G2(MP2) (25)[c]			0.95	0.89	1.12		0.87	0.85
slope vs G2(MP2) (12)[c]			0.92	0.98	1.23		0.88	0.84

[a] Relative energies are in kcal/mol and include scaled zero-point energy corrections (see text). The ranking of conformers is based on the B3LYP/6-31+G**//HF/6-31G* energy. See Supporting Information for all 75 conformers. [b] Structures that are unique to the HF/6-31G* conformer set. [c] Number of lowest energy conformers used.

formations, namely $\alpha\alpha$, $\alpha\beta$, $\alpha\gamma$, $\beta\beta$, $\beta\gamma$, and $\gamma\gamma$ (ignoring prochiral partners for $\alpha\beta$, $\beta\gamma$, and $\alpha\gamma$). Each backbone conformation may in turn exhibit a different preferential arrangement of the hydroxyl hydrogens.

Glycerol has been studied in the gas phase by a variety of different methods including electron diffraction[12a] and microwave spectroscopy.[12b] The electron diffraction studies indicate that the major backbone conformations for gaseous glycerol are the $\alpha\alpha$ and $\alpha\gamma$ structures. The microwave spectroscopic studies indicate that the $\gamma\gamma$ backbone shown in Table 1 (structure **100**, Figure 4) is present in a mixture with the $\alpha\gamma$ forms. Theoretical studies on glycerol have also been performed in the gas phase. These ab initio[16] studies on an isolated glycerol molecule agree with the microwave studies and indicate that the $\gamma\gamma$ conformation is the most energetically favorable. However, in all of the previous ab initio investigations of glycerol, only a small portion of the conformational energy surface has been sampled, and the largest number of distinct conformations which have been studied is 13.[16] More recent density functional theory (B3LYP/6-31G*) investigations[17] have been coupled with IR spectroscopic studies and have indicated that conformers **100** and **95** (Figure 4), respectively, are the most stable in the gas phase. However, we[6] and others[18−20] have shown that the relative

(16) (a) van Den Enden, L.; van Alsenoy, C.; Scarsdale, J. N.; Schäfer, L. *THEOCHEM* **1983**, *104*, 471. (b) van Alsenoy, C.; Klimkowski, V. J.; Ewbank, J. D.; Schäfer, L. *THEOCHEM* **1985**, *121*, 153. (c) Teppen, B. J.; Cao, M.; Frey, R. F.; van Alsenoy, C.; Miller, D. M.; Schäfer, L. *THEOCHEM* **1994**, *120*, 169. (d) Chelli, R.; Procacci, P.; Cardini; G.; Califano, S. *Phys. Chem. Chem. Phys.* **1999**, *1*, 879. (e) Chelli, R.; Procacci; P.; Cardini, G.; Della Valle, R. G.; Califano, S. *Phys. Chem. Chem. Phys.* **1999**, *1*, 871.

(17) (a) Chelli, R.; Gervasio, F. L.; Gellini, C.; Procacci, P.; Cardini, G.; Schettino, V. *J. Phys. Chem. A* **2000**, *104*, 5351. (b) Chelli, R.; Gervasio, F. L.; Gellini, C.; Procacci, P.; Cardini, G.; Schettino, V. *J. Phys. Chem. A* **2000**, *104*, 11220.

(18) (a) Csonka, G. I.; Éliás, K.; Csizmadia, I. G. *J. Comput. Chem.* **1997**, *18*, 330. (b) Csonka, G. I.; Éliás, K.; Kolossváry, I.; Sosa, C. P.; Csizmadia, I. G. *J. Phys. Chem. A* **1998**, *102*, 1219. (c) Csonka, G. I.; Kolossváry, I.; Császár, P.; Éliás, K.; Csizmadia, I. G. *THEOCHEM* **1997**, *395*, 29. (d) Csonka, G. I.; Sosa, C. P. *J. Phys. Chem. A* **2000**, *104*, 7113. (e) Csonka, G. I.; Sosa, C. P.; Csizmadia, I. G. *J. Phys. Chem. A* **2000**, *104*, 3381.

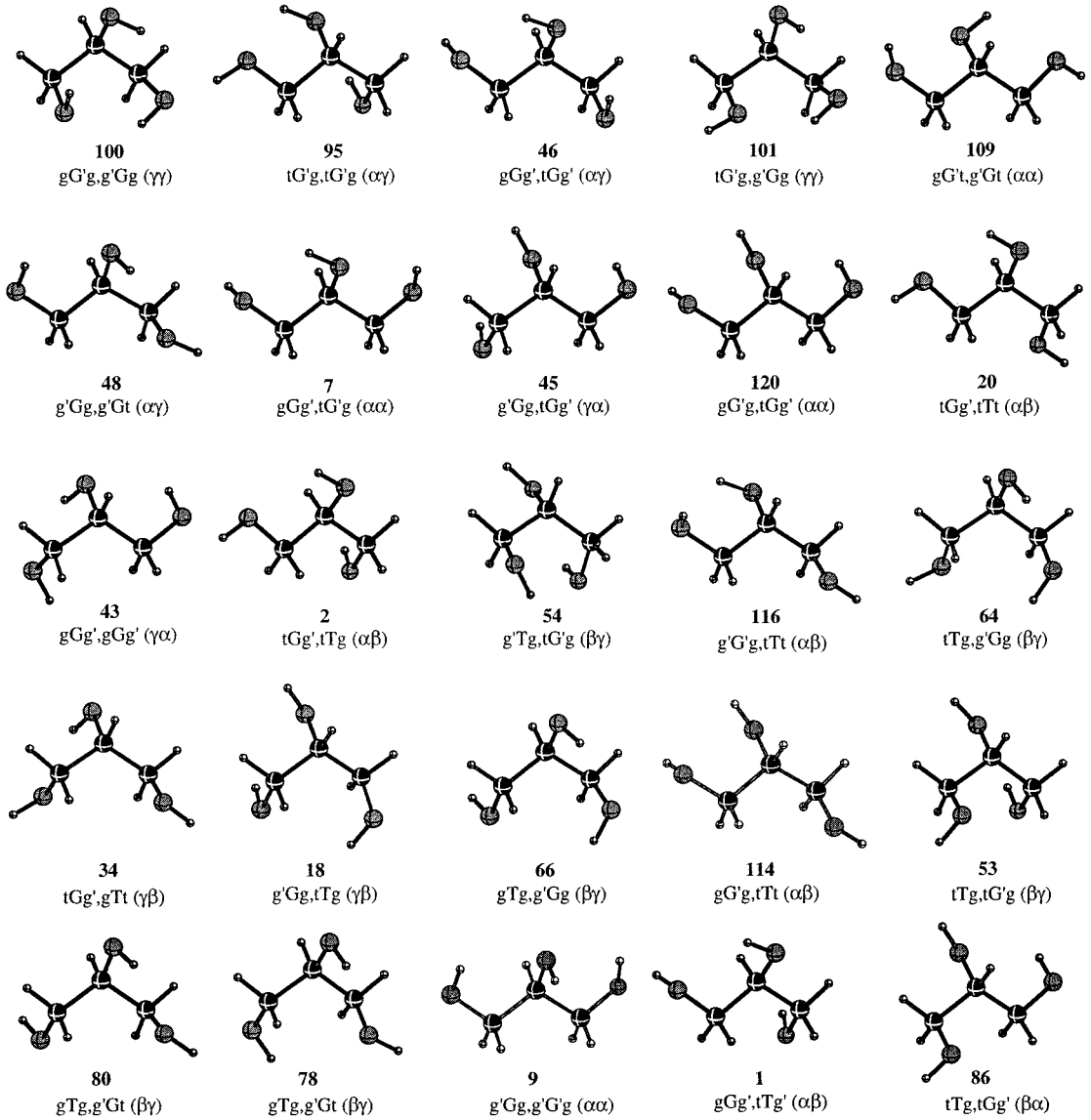

Figure 4. The lowest energy conformations of glycerol at the G2(MP2) level of theory using the MP2(full)/6-31G* geometries.

energies between conformers with intramolecular hydrogen bonds at this level of theory can be in error. Also, the role of enthalpic and entropic contributions to the Gibbs free energy may be important for these systems. In a recent paper,[17b] Procacci and co-workers combined DFT and statistical mechanics calculations to determine the conformational distribution of gas-phase glycerol on a limited number of conformations at different temperatures. Their results agreed with infrared spectroscopic and electron diffraction measurements and are also in agreement with previous molecular dynamics simulation data.[16d,e] However, a question remains as to the accuracy of their Boltzmann distribution, given the limited number of conformations that were investigated.

The conformation of glycerol in aqueous solution has also been reported. In a series of neutron scattering experiments,[13] the $\alpha\alpha$ and $\alpha\gamma$ conformations were used to explain the observed structure factors. In a ^{1}H NMR study,[21] the aqueous-phase conformers were determined in D_2O at various temperatures. These aqueous solution studies determined that the $\alpha\alpha$, $\alpha\beta$, $\alpha\gamma$, and $\beta\gamma$ backbone conformations were present in greater percentages than the $\beta\beta$ and $\gamma\gamma$ backbones.

To shed further light on the structural properties of glycerol in the gas and aqueous phases, we have conducted a systematic series of ab initio molecular orbital and density functional theory optimizations of all of the possible staggered conformers of glycerol and have calculated the Boltzmann distributions in the gas and aqueous phases. In addition to gaining a better understanding of the favored conformations of glycerol in these different phases, we are interested in evaluating reliable and accurate computational methods for molecules which possess strong intramolecular hydrogen-bonding interactions. Glycerol is an ideal model system to study the importance of different types of intramolecular hydrogen-bonding patterns. Because of the small size of the molecule, very accurate quantum-mechanical methods can be used to determine the basis set and the level of theory needed to obtain accurate relative energies and geometries of these systems, especially with respect to the importance of hydrogen-bonding interactions.

(19) (a) Ma, B.; Schaefer, H. F., III; Allinger, N. L. *J. Am. Chem. Soc.* **1998**, *120*, 3411. (b) Lii, J. H.; Ma, B. Y.; Allinger, N. L. *J. Comput. Chem.* **1999**, *20*, 1593.

(20) Del Bene, J. E.; Person, W. B.; Szczepaniak, K. *J. Phys. Chem.* **1995**, *99*, 10705.

(21) Van Koningsveld, H. *Recl. Trav. Chim. Pays-Bas.* **1970**, *89*, 801. While this report from 1970 was performed with a 220 MHz NMR spectrometer, we have independently confirmed the original results with a 500 MHz NMR spectrometer and the coupling constants are identical.

II. Theoretical Methods

A. General Methods. Ab initio molecular orbital[22] and density functional theory (DFT)[23] calculations for glycerol were performed using Gaussian 98.[24] The optimized geometries were calculated at the HF/6-31G* and B3LYP/6-31G* levels of theory.[25] Single-point energies of these optimized geometries were determined at the CCSD/6-31+G**,[26] CCSD(T)/6-31+G**,[27] B3LYP/6-31+G**, and B3LYP/6-311+G(3df,2p) levels. As the latter two methods should be applicable to larger carbohydrates, the studies reported here will provide calibration for the accuracy of these different theoretical levels for molecules with extensive intramolecular hydrogen bonding. Calibration calculations were also performed at the G2(MP2)[28] and CBS-QB3[29] levels of theory.

Each stationary point was verified to be a minimum or saddle point via a vibrational frequency analysis. The zero-point vibrational energies (ZPEs) were scaled by a factor of 0.9135 for the HF/6-31G* structures and 0.9806 for the B3LYP/6-31G* geometries.[30] The vibrational frequency analyses also provided thermal corrections to the enthalpy and entropy, which allowed the determination of the relative free energies at 298 K. The overall Gibbs free energy at each temperature was calculated by adding the single-point energy, the scaled ZPE, and the thermodynamic contribution to the free energy (as well as the degeneracy of the conformer). The Boltzmann distribution was determined from the relative free energies of the conformers. The ZPE scaling factor used for the G2 method (for a HF/6-31G* geometry) is 0.8929.[28] The ZPE scaling factor used for the CBS-QB3 method (for a B3LYP/6-311G(2d) geometry) is 0.9986.[29] The geometrical data for all conformations were analyzed using the ConforMole program.[31]

B. Protocol for Conformer Generation. The 486 conformers of glycerol were reduced to 126 symmetry-distinct representatives by first constructing a skeleton for each structure with fixed bond lengths and perfect tetrahedral bond angles. The list of intramolecular distances within the skeleton provides a consistent criterion for detecting symmetry-redundant structures, because both enantiomeric conformations and conformations related by rotation have identical lists. The Maple symbolic algebra program was used to program these operations.[32] Efficient algorithims for eliminating symmetry-related structures have been described elsewhere.[33,34]

C. Gas-Phase Calculations. Complete geometry optimizations were performed for all 126 conformational isomers at the HF/6-31G* level by a partial optimization of all parameters (e.g., bond lengths, bond angles) except the five dihedral angles used to define each conformation. A second calculation was subsequently performed removing the dihedral constraints, and the resulting geometries were compared using ConforMole to determine the diversity of the conformer set generated. This two-step optimization method was used to ensure that the largest diversity of conformations would be found. For each of these steps, analytical second derivatives were used. After these two optimizations, B3LYP/6-31+G**, B3LYP/6-311+G(3df,2p), CCSD/6-31+G**, and CCSD(T)/6-31+G** single-point energies were calculated for each conformer. The HF/6-31G* geometries were also used as starting geometries for the G2(MP2) calculations.

A similar analysis was performed using all of the 126 possible conformational isomers at the B3LYP/6-31G* level. After these two optimizations, single-point energies were calculated with the B3LYP/6-31+G**, B3LYP/6-311+G(3df,2p), CCSD/6-31+G**, and CCSD(T)/6-31+G** levels. The B3LYP/6-31G* geometries were further used as input geometries for the CBS-QB3 calculations.

D. Aqueous-Phase Calculations. Aqueous-phase calculations were performed using the MN-GSM (Minnesota Gaussian Solvation Module, version 99.2) at the SM5.42/HF/6-31G* level of theory.[10] Upon gas-phase HF/6-31G* optimization of the 126 initial glycerol structures, 75 unique conformers resulted (see later), and these were further refined using the SM5.42 solvation model. The aqueous-phase B3LYP/6-31+G**//SM5.42/HF/6-31G* single-point energies of these conformations were determined according to eqs 1 and 2 from the gas-phase HF/6-31G* and B3LYP/6-31+G** single-point energies of the aqueous-phase geometries.

$$\Delta E_{\text{solvation}} = E_{\text{SM5.42/HF/6-31G*}} - E_{\text{HF/6-31G*}}(\text{gas}) \quad (1)$$

$$E_{\text{B3LYP/6-31+G**//SM5.42/HF/6-31G*}}(\text{aq}) = E_{\text{B3LYP/6-31+G**(gas)//SM5.42/HF/6-31G*}} + \Delta E_{\text{solvation}} \quad (2)$$

We also attempted to use the PCM[35] and CPCM[36] solvation models, but some difficulties were experienced in optimizing all of the conformations (see Supporting Information).

III. Results and Discussion

A. Gas-phase ab Initio Geometries. The results of the HF/6-31G* optimizations are reported in Table 1, together with the relative energies of the G2(MP2) calculations and numerous single-point energies. In Table 1, the structures are rank-ordered based on their B3LYP/6-31+G**//HF/6-31G* relative energies. Upon optimization of the 126 starting geometries, 75 unique conformers were obtained. As can be seen, conformations **100** (gG′g,g′Gg) and **95** (tG′g,tG′g) are of the lowest energy at all levels of theory. Figure 4 illustrates some of the important low-energy optimized structures of the conformers of glycerol at the G2(MP2) level of theory. Additional geometric and energetic details for all of the optimized conformers are provided in the Supporting Information. Conformer **95** is the lowest energy structure at the HF/6-31G* level of theory by 0.27 kcal/mol. To evaluate the effect of basis set, we used the HF/6-31G*

(22) Hehre, W. J.; Radom, L.; Schyeyer, P. v. R.; Pople, J. A. *Ab initio Molecular Orbital Theory*; John Wiley & Sons: New York, 1986.

(23) (a) Labanowski, J. W.; Andzelm, J. *Density Functional Methods in Chemistry*; Springer: New York, 1991. (b) Parr, R. G.; Yang, W. *Density Functional Theory in Atoms and Molecules*; Oxford University Press: New York, 1989.

(24) Frisch, M. J.; Trucks, G. W.; Schlegel, H. B.; Scuseria, G. E.; Robb, M. A.; Cheeseman, J. R.; Zakrzewski, V. G.; Montgomery, J. A., Jr.; Stratmann, R. E.; Burant, J. C.; Dapprich, S.; Millam, J. M.; Daniels, A. D.; Kudin, K. N.; Strain, M. C.; Farkas, O.; Tomasi, J.; Barone, V.; Cossi, M.; Cammi, R.; Mennucci, B.; Pomelli, C.; Adamo, C.; Clifford, S.; Ochterski, J.; Petersson, G. A.; Ayala, P. Y.; Cui, Q.; Morokuma, K.; Malick, D. K.; Rabuck, A. D.; Raghavachari, K.; Foresman, J. B.; Cioslowski, J.; Ortiz, J. V.; Stefanov, B. B.; Liu, G.; Liashenko, A.; Piskorz, P.; Komaromi, I.; Gomperts, R.; Martin, R. L.; Fox, D. J.; Keith, T.; Al-Laham, M. A.; Peng, C. Y.; Nanayakkara, A.; Gonzalez, C.; Challacombe, M.; Gill, P. M. W.; Johnson, B. G.; Chen, W.; Wong, M. W.; Andres, J. L.; Head-Gordon, M.; Replogle, E. S.; Pople, J. A. *Gaussian 98*, revision A.9; Gaussian, Inc.: Pittsburgh, PA, 1998.

(25) (a) Becke, A. D. *Phys. Rev. A* **1998**, *38*, 3098. (b) Becke, A. D. *J. Chem. Phys.* **1993**, *98*, 5648. (c) Lee, C.; Yang, W.; Parr, R. G. *Phys. Rev. B* **1988**, *37*, 785. (d) Stevens, P. J.; Devlin, F. J.; Chabalowski, C. F.; Frisch, M. J. *J. Phys. Chem.* **1994**, *98*, 1623.

(26) (a) Bartlett, R. J.; Purvis, G. D. *Int. J. Quantum Chem.* **1978**, *14*, 561. (b) Purvis, G. D.; Bartlett, R. J. *J. Chem. Phys.* **1982**, *76*, 1910. (c) Scuseria, G. E.; Janssen, C. L.; Schaefer, H. F., III. *J. Chem. Phys.* **1988**, *89*, 7382. (d) Scuseria, G. E.; Schaefer, H. F., III. *J. Chem. Phys.* **1989**, *90*, 3700.

(27) Lee, T. J.; Scuseria, G. E. *Quantum Mechanical Electronic Structure Calculations with Chemical Accuracy*; Langoff, S. F., Ed.; Kluwer Academic Press: Dordrecht, 1995.

(28) (a) Curtiss, L. A.; Raghavachari, K.; Pople, J. A. *J. Chem. Phys.* **1993**, *98*, 1293. (b) Curtiss, L. A.; Raghavachari, K.; Trucks, G. W.; Pople, J. A. *J. Chem. Phys.* **1991**, *94*, 7221.

(29) Montgomery, J. A., Jr.; Frisch, M. J.; Ochterski, J. W.; Petersson, G. A. *J. Chem. Phys.* **1999**, *110*, 2822.

(30) Scott, A. P.; Radom, L. *J. Phys. Chem.* **1996**, *100*, 16502.

(31) McCarren, P. R. *ConforMole*; The Ohio State University: Columbus, Ohio. This program is available upon request.

(32) *Maple*, 6.01; Waterloo Maple Inc., 2000.

(33) McDonald, S.; Ojamäe, L.; Singer, S. J. *J. Phys. Chem. A* **1998**, *102*, 2824.

(34) Kuo, J.-L.; Coe, J. V.; Singer, S. J.; Band, Y. B.; Ojamäe, L. *J. Chem. Phys.* **2001**, *114*, 2527.

(35) (a) Tomasi, J.; Persico, M. *Chem. Rev.* **1994**, *94*, 2027. (b) Miertus, S.; Scrocco, E.; Tomasi, J. *Chem. Phys.* **1981**, *55*, 117. (c) Cammi, R.; Tomasi, J. *J. Comput. Chem.* **1995**, *16*, 1449. (d) Cossi, M.; Barone, V.; Cammi, R.; Tomasi, J. *Chem. Phys. Lett.* **1996**, *255*, 327. (e) Amovilli, C.; Barone, V.; Cammi, R.; Cancés, E.; Cossi, M.; Mennucci, B.; Pommelli, C. S. *Adv. Quantum Chem.* **1998**, *32*, 227. (f) Cramer, C. J.; Truhlar, D. G. *Chem. Rev.* **1999**, *99*, 2161.

(36) (a) Barone, V.; Cossi, M. *J. Phys. Chem. A* **1998**, *102*, 1995. (b) Klamt, A.; Schueuermann, G. *J. Chem. Soc., Perkin Trans. 2* **1993**, 799.

Table 2. Relative Energies of Gas-Phase Conformers Calculated from B3LYP/6-31G* Geometries for the Lowest 26 Conformers[a]

conformer number	backbone	conformer	B3LYP/6-31G*	B3LYP/6-31+G** //B3LYP/6-31G*	B3LYP/6-311+ G(3df,2p) //B3LYP/6-31G*	CBS-QB3	CCSD/6-31+G** //B3LYP/6-31G*	CCSD(T) /6-31+G** //B3LYP/6-31G*
95	αγ	tG′g,tG′g	1.62	0.00	0.00	0.17	0.00	0.00
109	αα	gG′t,g′Gt	5.97	0.19	0.11	0.69	0.49	0.63
100	γγ	gG′g,g′Gg	0.00	0.64	0.51	0.00	0.86	0.50
46	αγ	gGg′,tGg′	1.51	0.69	0.46	0.75	0.98	0.87
101	γγ	tG′g,g′Gg	1.71	0.69	0.71	0.61	0.85	0.69
7	αα	gGg′,tG′g	2.53	0.82	0.55	1.22	1.34	1.35
48	αγ	g′Gg,g′Gt	2.57	0.92	0.79	1.09	1.14	1.13
120	αα	gG′g,tGg′	3.29	1.19	0.90	1.66	1.52	1.52
45	γα	g′Gg,tGg′	2.82	1.30	1.12	1.50	1.44	1.42
115[b]	αγ	tG′g,tTt	4.74	1.71	1.52	2.02	1.73	2.02
43	γα	gGg′,gGg′	2.57	1.75	1.37	1.72	2.35	2.19
2	αβ	tGg′,tTg	4.32	1.84	1.52	2.16	2.01	2.21
34	γβ	tGg′,gTt	4.60	1.88	1.61	1.88	1.80	2.00
116	αβ	g′G′g,tTt	4.26	1.95	1.62	2.21	2.18	2.35
9	αα	g′Gg,g′G′g	3.38	2.17	1.58	2.44	3.00	2.92
86	βα	tTg,tGg′	4.84	2.18	1.85	2.55	2.37	2.57
64	βγ	tTg,g′Gg	4.22	2.20	1.83	1.97	2.06	2.14
53	βγ	tTg,tG′g	4.53	2.28	1.86	2.23	2.22	2.37
80	βγ	gTg,g′Gt	4.43	2.32	1.93	2.33	2.43	2.52
1	αβ	gGg′,tTg	4.23	2.40	1.90	2.62	2.81	2.89
66	βγ	gTg,g′Gg	3.85	2.46	1.96	2.35	2.61	2.60
85	βα	gTg,tGg′	4.65	2.53	2.04	2.87	2.86	2.97
54	βγ	g′Tg,tG′g	4.07	2.54	2.22	2.15	2.15	2.17
75	ββ	g′Tg,tTt	4.60	2.57	2.42	2.97	2.82	2.91
83[b]	βγ	g′Tg,tG′g	4.08	2.58	2.26	2.12	2.18	2.19
78	βγ	gTg,g′Gt	4.80	2.75	2.46	2.33	2.35	2.41
av difference from CBS-QB3 (25)[c]			1.83	0.26	0.44		0.19	0.15
av difference from CBS-QB3 (12)[c]			1.75	0.28	0.44		0.26	0.15
slope vs CBS-QB3 (25)[c]			0.43	0.92	1.03		0.97	0.95
slope vs CBS-QB3 (12)[c]			0.26	1.06	1.21		0.94	0.95

[a] Relative energies are in kcal/mol and include scaled zero-point energy corrections (see text). The ranking of conformers is based on the B3LYP/6-31+G**//B3LYP/6-31G* energy. See the Supporting Information for all 76 conformers. [b] Structures that are unique to the B3LYP/6-31G* conformer set. [c] Number of low energy conformers included in calculation.

geometries and performed single-point energy calculations at the B3LYP/6-31+G** and B3LYP/6-311+G(3df,2p) levels. Upon performing these calculations, the same global minimum was observed but with a small decrease in relative energy between conformers **95** and **100**, to 0.22 and 0.15 kcal/mol, respectively. Furthermore, the relative energy differences between all of the conformations decrease as the size of basis set increases and electron correlation is included.

While the G2(MP2) method is currently impractical for an oligosaccharide, this level for glycerol can provide some quantitative verification of the more practical DFT levels. Therefore, G2(MP2) calculations were performed for each conformer. At this level, the relative energetic ordering between conformers **95** and **100** was inverted, and the latter became the global minimum. Conformer **95** is 0.21 kcal/mol higher in energy than **100** at the G2(MP2) level. Comparison of the G2(MP2) results to the more practical methods can be done with the data presented in Table 1. First, the inexpensive HF/6-31G* method does an impressive job of reproducing the G2(MP2) results for the lowest 25 conformers. This efficiency of the HF/6-31G* level has been noted earlier.[37] The B3LYP/6-31+G**//HF/6-31G* energies also provide excellent agreement for a number of conformations (up to 75) but are particularly effective for the 12 most stable conformers. Relative to the G2(MP2) results, the average difference over the range of (all 75) conformations for the B3LYP/6-31+G** single-point energies is 0.35 kcal/mol. The linear correlation (see Table 1) is the best observed for the conformational distribution. More impressively, for the 12 lowest energy conformers, the average energy difference relative to the G2(MP2) method is only 0.17 kcal/mol.

The CCSD/6-31+G** and CCSD(T)/6-31+G** single-point energy calculations were also performed on the 25 lowest energy conformers. The CCSD calculations also seem to do a reasonable job of predicting the relative stability of these conformers in the gas phase in comparison to the G2(MP2) level, but the CCSD and CCSD(T) calculations are far more expensive in comparison to the B3LYP method and therefore less applicable to much larger systems. The CCSD(T) and G2(MP2) calculations agree reasonably well for the low energy conformational isomers.

For the 12 lowest energy conformers, the correlation of the B3LYP/6-31+G**//HF/6-31G* energies to the G2(MP2) values has a slope of 0.98 and is the best for the levels considered here (see Table 1 and Supporting Information).

B. Gas-Phase Density Functional Theory Geometries. The results of the B3LYP/6-31G* geometry optimizations are reported in Table 2, along with the relative energies of the CBS-QB3 calculations and B3LYP/6-31+G**, B3LYP/6-311+G(3df,2p), CCSD/6-31+G**, and CCSD(T)/6-31+G** single-

(37) (a) Barrows, S. E.; Storer, J. W.; Cramer, C. J.; French, A. D.; Truhlar, D. G. *J. Comput. Chem.* **1998**, *19*, 1111. (b) Barrows, S. E.; Dulles, F. J.; Cramer, C. J.; French, A. D.; Truhlar, D. G. *Carbohydr. Res.* **1995**, *276*, 219. (c) French, A. D.; Kelterer, A.-M.; Johnson, G. P.; Dowd, M. K.; Cramer, C. J. *J. Comput. Chem.* **2001**, *22*, 65. (d) French, A. D.; Kelterer, A.-M.; Cramer, C. J.; Johnson, G. P.; Dowd, M. K. *Carbohydr. Res.* **2000**, *326*, 305.

(38) (a) Sheppard, N.; Turner, J. J. *Proc. R. Soc. London.* **1959**, *A252*, 506. (b) Gutowsky, H. S.; Belford, G. G.; McMahon, P. E. *J. Chem. Phys.* **1962**, *36*, 3353.

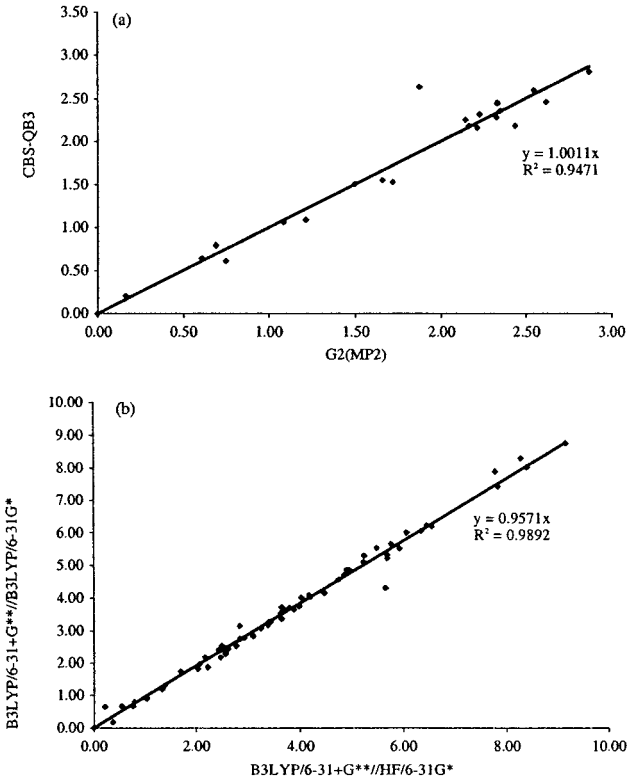

Figure 5. (a) G2(MP2) relative energies vs CBS-QB3 relative energies. (b) B3LYP/6-31+G**//HF/6-31G* relative energies vs B3LYP/6-31+G**//B3LYP/6-31G* relative energies.

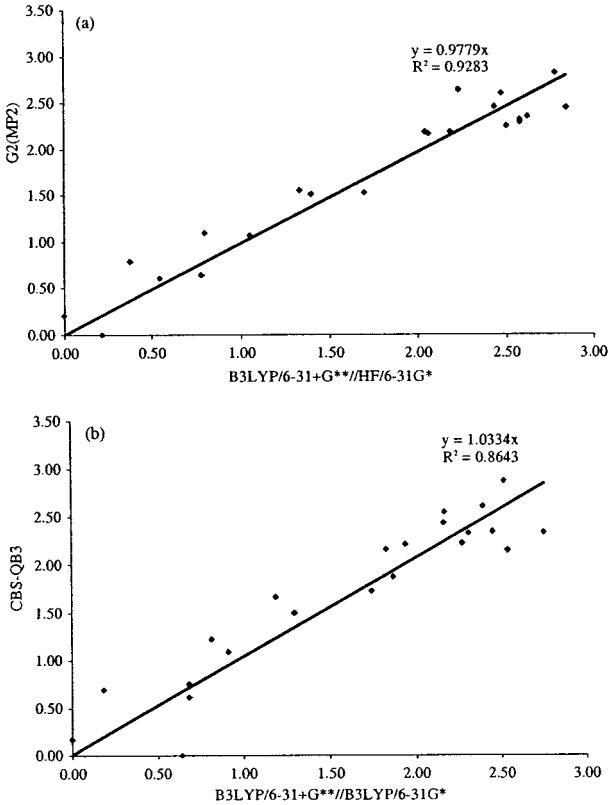

Figure 6. (a) B3LYP/6-31+G**//HF/6-31G* relative energies vs G2(MP2) relative energies. (b) B3LYP/6-31+G**//B3LYP/6-31G* relative energies vs CBS-QB3 relative energies.

point energies. Minimization of the 126 starting structures provided 77 unique conformers. As can be seen in Table 2, the conformational energy distribution is broader when using DFT geometries. For most levels of theory, conformations **100**, **109**, and **95** are predicted to be the lowest energy conformers. Energies derived from the B3LYP/6-31G* level are significantly different when compared to those from the CBS-QB3 level. The B3LYP/6-31G* optimization predicted conformer **100** to be the global minimum by 1.51 kcal/mol over conformer **46**. However, single-point energies derived at the B3LYP/6-31+G** and B3LYP/6-311+G(3df,2p) levels predict that the global minimum is conformer **95** by 0.19 and 0.11 kcal/mol, respectively, over conformer **109**. These data demonstrate the poor energies associated with the B3LYP/6-31G* level for compounds with strong nonbonded interactions such as intramolecular hydrogen bonds. This effect has been noted previously by us[6] and others.[18−20] As the basis set size is increased, the B3LYP/6-31+G** and B3LYP/6-311+G(3df,2p) single-point energies show that the relative energies between the different conformations decrease and more accurately predict the correct relative energetics as compared to the CBS-QB3 level.

The CBS-QB3 level of theory does predict that conformations **100** and **95** are the lowest energy geometries (Table 2). We note that all of the other single-point energies (including scaled ZPE corrections) do predict the incorrect global minimum (by 0.5 kcal/mol) relative to the CBS-QB3 level.

When comparing the CBS-QB3 energies with the B3LYP single-point energies, one of the best comparisons over the entire conformational distribution is at the B3LYP/6-31+G**//B3LYP/6-31G* level which has an average absolute difference of 0.27 kcal/mol and a linear correlation of 0.92 to the CBS-QB3 level (Table 2). The larger B3LYP/6-311+G(3df,2p) single-point energy calculations also showed a good correlation with the CBS-QB3 energies, but the average absolute deviation is slightly larger. The CCSD and CCSD(T) single-point energies showed excellent correlation to the CBS-QB3 energies with a small absolute energy difference of less than 0.2 kcal/mol and an average linear correlation of 0.95.

C. Conformational Description of the Low Energy Structures in the Gas Phase. Conformer **100** is the only form of glycerol which possesses three intramolecular hydrogen bonds (see Figure 4). The hydrogen bonds form three rings within the molecule: one is a chair-type, six-membered ring and the other two are five-membered rings that each share a C−C bond with this six-membered ring. Conformer **95** has two intramolecular hydrogen bonds and is essentially composed of two units of the global minimum that was described earlier for 1,2-ethanediol (ethylene glycol), **A**, by Cramer and Truhlar.[11a] For **95**, there are two adjacent five-membered rings arranged on an $\alpha\gamma$ backbone. These *geometrical* trends are reproduced by the HF and B3LYP potential energy surfaces. However, the B3LYP/6-31G* density functional theory method does overestimate the *energetic* importance of the hydrogen-bonded interactions as noted previously. In the case of **95**, the higher levels of theory may overestimate the steric repulsion between H_8 and C_3 along the $H_8-O_6-C_2-C_3$ dihedral angle (see Figures 1 and 4), which is 19.4°. However, there seems to be a balance between the stability of the backbone in conformer **95** versus the backbone in conformation **100**, but the energetic benefit due to three hydrogen bonds favors **100**. The other low-energy conformations are shown in Table 1 and Figure 4. While only the G2(MP2) structures are shown, the numbers used throughout this discussion are uniform so that conformation **100** for all levels of theory has the same backbone and hydrogen-bonding orientation.

D. Comparison of Energy Distribution between HF and DFT Levels of Theory in the Gas Phase. It was of initial concern to us that certain structures in the gas phase would not

Table 3. Relative Energies of Aqueous Solution Conformers Calculated for the SM5.42/HF/6-31G* Geometries[a]

conformer number	backbone	conformer	SM5.42/HF /6-31G*	B3LYP/6-31 +G**//SM5.42 /HF/6-31G*	conformer number	backbone	conformer	SM5.42/HF /6-31G*	B3LYP/6-31 +G**//SM5.42 /HF/6-31G*
95	αγ	tG′g,tG′g	0.00	0.10	**108**	αγ	g′G′g,tG′t	1.73	1.21
46	αγ	gGg′,tGg′	0.17	0.02	**41**	γγ	g′Gg,tG′g′	1.74	1.33
45	γα	g′Gg,tGg′	0.36	0.18	**3**	αβ	g′Gg,g′Tg	1.79	1.50
109	αα	gG′t,g′Gt	0.43	0.03	**28**	γα	tGg,tGg′	1.85	1.44
100	γγ	gG′g,g′Gg	0.60	0.48	**70**	ββ	gTg,g′Tt	2.08	2.14
48	αγ	g′Gg,g′Gt	0.62	0.39	**110**	αα	tG′g,tGt	2.10	1.30
7	αα	gGg′,tG′g	0.64	0.00	**55**	ββ	gTg,g′Tg	2.13	2.27
86	βα	tTg,tGg′	0.68	0.69	**83**	βγ	g′Tg,tG′g′	2.28	2.67
20	αβ	tGg′,tTt	0.77	1.04	**69**	βγ	g′Tg,tG′t	2.28	2.64
101	γγ	tG′g,g′Gg	0.83	0.62	**31**	αγ	tGg,g′Gt	2.29	1.90
35	γβ	g′Gg,tTt	0.85	1.25	**111**	αα	g′G′gtGt	2.29	1.30
116	αβ	g′G′g,tTt	0.88	1.04	**17**	γβ	tGg,tTg	2.32	2.78
18	γβ	g′Gg,tTg	0.88	1.54	**12**	γα	g′Gg,tGg	2.34	1.87
85	βα	gTg,tGg′	0.90	0.82	**38**	αβ	g′Gg,g′Tg′	2.34	1.81
120	αα	gG′g,tGg′	0.92	0.16	**117**	αγ	tG′g,tG′g′	2.41	1.89
53	βγ	tTg,tG′g	0.95	1.28	**98**	αα	tG′g,tGg′	2.41	1.58
2	αβ	tGg′,tTg	0.96	1.19	**33**	γβ	gGg,tTt	2.41	2.92
51	γβ	g′G′g,tTg′	0.98	1.20	**82**	βγ	tTg,tG′g′	2.44	2.79
54	βγ	g′Tg,tG′g	0.98	1.56	**119**	αγ	g′G′g,tG′g′	2.50	1.82
52	βγ	gTg,tG′g	1.05	1.19	**81**	βγ	gTg,tG′g′	2.57	2.80
34	γβ	tGg′,gTt	1.10	1.46	**49**	γβ	gGg,tTg′	2.59	2.98
64	βγ	tTg,g′Gg	1.11	1.59	**68**	βγ	tTg,tG′t	2.61	2.73
1	αβ	gGg′,tTg′	1.13	1.18	**99**	γγ	g′G′g,tGg	2.63	1.54
80	βγ	gTg,g′Gt	1.18	1.46	**67**	βγ	gTg,tG′t	2.66	2.60
43	γα	gGg′,gGg′	1.20	0.73	**59**	βα	tTg,tGg	2.84	2.60
78	βγ	gTg,g′Gt	1.20	1.67	**14**	αγ	tGg,g′Gg	3.03	2.36
75	ββ	g′Tg,tTt	1.24	1.88	**58**	βα	gTg,tGg	3.09	2.69
66	βγ	gTg,g′Gg	1.27	1.69	**40**	γγ	tGg,tG′g′	3.14	2.31
88	ββ	g′Tg,tTg′	1.32	1.91	**60**	βα	g′Tg,tGg	3.61	3.18
9	αα	g′Gg,g′G′g	1.43	0.46	**11**	γα	tGg,tGg	3.82	3.07
103	αβ	gG′t,g′Tg	1.45	1.35	**112**	γγ	gG′g,g′Gt	3.87	3.62
114	αβ	gG′g,tTt	1.47	1.53	**113**	γγ	tG′g,g′Gt	4.22	3.72
21	αβ	g′Gg,g′Tt	1.59	1.24	**27**	γα	gGg,tGt	4.56	4.33
106	αγ	tG′g,tG′t	1.59	1.27	**26**	αα	tGg,g′G′t	4.77	3.49
62	ββ	tTg,tTg	1.60	2.06	**123**	γγ	gG′g,g′Gg′	5.05	4.27
61	ββ	gTg,tTg	1.61	2.05	**71**	ββ	tTg,g′Tt	5.89	5.72
104	αβ	tG′g,tTg	1.62	1.64	**57**	ββ	g′Tg,g′Tg	5.97	6.05
105	αβ	g′G′g,tTg	1.70	1.61					

[a] Relative energies are in kcal/mol and do not include a ZPE correction.

be found by both HF and DFT methods. However, the HF/6-31G* and B3LYP/6-31G* conformations are essentially identical geometries with regard to the general orientation of dihedral angles for the same conformer number. The conformational distribution between the HF and B3LYP levels were identical as far as backbones and hydrogen-bonding arrays to 89%. Furthermore, of those structures that were not found by both HF/6-31G* (7) and B3LYP/6-31G* (10) methods, only one structure in each set was of low energy (within 2 kcal/mol of the global minimum), and each was a minor contributor to the respective Boltzmann population. Furthermore, the relative energies at the G2(MP2) and CBS-QB3 levels are in excellent agreement (Figure 5a). The slope of the plot which correlates the CBS-QB3 and G2(MP2) energies for the lowest 25 conformations is 1.001 with a correlation coefficient (R^2) of 0.95. Below 2 kcal/mol, there is an excellent correspondence between the levels. There is similar excellent agreement between B3LYP/6-31+G** single-point energies based on either HF/6-31G* or B3LYP/6-31G* geometries (Figure 5b). The slope for this correlation is 0.96 with an R^2 value of 0.99. This suggests that B3LYP/6-31+G** single-point energies on either HF/6-31G* or B3LYP/6-31G* geometries are very good for obtaining accurate gas-phase relative energies. Figure 6 presents the linear correlations of the B3LYP/6-31+G**//HF/6-31G* versus G2(MP2) levels with slope = 0.98, R^2 = 0.93 (Figure 6a), and B3LYP/6-31+G**//B3LYP/6-31G* versus CBS-QB3 levels with slope = 1.03, R^2 = 0.86 (Figure 6b).

E. Aqueous-Phase Calculations. The results of the SM5.42/HF/6-31G* calculations are reported in Table 3, along with the relative B3LYP/6-31+G**//SM5.42/HF/6-31G* energies. The energies in Table 3 do not include ZPE energy corrections. (The relative energies including the scaled ZPE corrections can be found in Supporting Information.)

As can be seen from the data in Table 3, conformations **95** and **46** are the lowest energy conformers when solvation is included. In aqueous solution, conformation **100** which was the global minimum at multiple levels of theory in the gas phase is now 0.60 kcal/mol higher in energy than the global minimum with solvation. Conformer **100** is of higher relative energy, because all three hydroxyl groups are involved in an intramolecular hydrogen-bonding array and are, hence, unavailable to interact with the solvent. It is important to stress that many structures that possess intramolecular hydrogen-bonding arrays (e.g., **95**, **46**, **101**, **109**) are still low-energy conformations in aqueous solution, even when compared to structures which do not possess any intramolecular hydrogen bonds (e.g., **123**, **71**, **57**). These results suggest that a combination of intramolecular hydrogen bonds and intermolecular solvation of hydroxyl groups stabilizes glycerol in aqueous solution. A similar decrease in intramolecular hydrogen bonding (but not an elimination of)

Table 4. Hydrogen-Bond Lengths and Angles at Different Levels of Theory[a]

	HF/6-31G*	G2(MP2)[d]	B3LYP /6-31G*	CBS-QB3	SM5.42 /HF/6-31G*
			Bond Lengths[b]		
average	2.34	2.21	2.24	2.26	2.51
maximum	2.80	2.70	2.80	2.87	2.95
minimun	2.04	1.93	1.96	1.98	2.09
			Bond Angles[c]		
average	110.6	116.7	116.9	115.2	106.9
maximum	137.8	142.2	142.3	137.5	137.6
minimun	85.5	100.3	100.9	101.6	83.8

[a] Distance between the hydrogen-bond donor (H) and acceptor (O). [b] Bond lengths are in angstroms. [c] Bond angles are in degrees. [d] Using the MP2 geometries.

was noted in an earlier theoretical study on ethylene glycol (**A**, Chart 1) and in other systems.[11a,37b] For polyhydroxylated systems, these results also suggest that attempting to improve the agreement between gas-phase calculations and aqueous-phase experimental data will not be possible simply by biasing such systems against the formation of intramolecular hydrogen bonds. This is consistent with previous work from our laboratories on the conformations of methyl α-D-arabinofuranoside.[7]

Comparing the relative energies listed in Tables 1−3, it is clear that the ordering of the higher energy structures in both the gas and aqueous phases are similar, but in the aqueous phase, the relative energy differences have decreased by an average of 2 kcal/mol over all levels of theory. That is, the relative energy range has been quite compressed. *However, the low-energy conformations in the gas phase are similar to those in aqueous solution with a preference for certain structures in the gas phase that possess favorable backbones and hydrogen-bonding arrays*.

F. Comparison of Geometrical Data with Different Level of Theory. Geometrical data for all of the conformations (e.g., bond lengths, bond angles, dihedral angles, and hydrogen-bonding distances and angles) can be found in the Supporting Information. Table 4 shows the average hydrogen-bonding lengths and angles for the various levels of theory which were used. The HF/6-31G* hydrogen-bond lengths are on average 5.4% longer than the MP2 bond lengths from the G2(MP2) level, and the B3LYP/6-31G* hydrogen bond lengths are 1% shorter than those at the CBS-QB3 level. Overall for the SM5.42/HF/6-31G* geometries, the average hydrogen-bond length is 2.52 Å which is larger (6.9%) than that for the HF/6-31G* geometries. In the solution-phase conformations, there is also a slight decrease in the average hydrogen-bond angle. As detailed in the Supporting Information, on going from the gas to the aqueous phase, there is a significant increase in the length of O−H bonds that serve as hydrogen-bond donors. The O−H bonds that are not involved in intramolecular hydrogen bonding have lengths similar to those of the gas-phase structures. A comparison of the average bond distances and hydrogen-bonding interactions can be seen in Tables 4 and 5. The dipole moments (Supporting Information) of the different conformations do not appear to show any correlation to their energetic stability. For the aqueous solvation model, the low-energy conformations have shifted to favor the αα or αγ backbone orientation, while those conformations with the γγ backbone, which are favored in the gas phase, have correspondingly increased in energy.

Table 5 depicts the average bond lengths for all of the bonds in glycerol. For the various levels of theory, the nonbonded interactions (i.e., hydrogen bonding) change depending on the inclusion of electron correlation. HF procedures overlocalize the electrons in the bonding regions;[22] therefore, the HF-optimized bond distances are too short, and nonbonded separations are too long. When the MP2 or B3LYP geometries are used, optimizations produce O−H bonds that were longer. Also, the combined effects of changes in the bond length, bond angle, and dihedral angle with the inclusion of electron correlation effectively decrease the hydrogen-bonding interaction as compared to the HF geometries. Furthermore, the geometric trends over all of the conformers for each level of theory are within reasonable agreement. This illustrates that HF/6-31G* and B3LYP/6-31G* calculations can accurately predict the structural trends, even though they are not able to evaluate the nonbonding and bonding interaction distances as accurately.

IV. Comparison to Experimental Boltzmann Distribution and Free Energy Calculations

The relative free energies and Boltzmann distributions were calculated for all of the conformations studied at each level of theory. The conformer distributions are shown in Tables 6 and 7, and these results are compared below to the available experimental data.

A. Electron Diffraction Gas-Phase Studies. A seminal investigation of the conformation of glycerol[12a] in the gas phase by electron diffraction suggested that the most likely configurations present are the αα and αγ backbones (on the basis of the anticipated backbone configurations and stabilities formed by intramolecular hydrogen bonds). The average hydrogen-bonding distance measured from these studies is 2.96 ± 0.02 Å. On the basis of further calorimetric data presented in the same paper, it was suggested that most of the structures present have two intramolecular hydrogen bonds.

The gas-phase Boltzmann distributions (298 K) calculated by us at the ab initio and DFT levels of theory are in good agreement with this study. As can be seen in Tables 6 and 7, conformers with the αγ backbone are the major contributors to the Boltzmann distribution at all levels of theory, except at the B3LYP/6-31G* level. The conformers with the αα backbone are also major contributors to the Boltzmann population at all levels of theory. For example, on the basis of the B3LYP/6-31+G**//HF/6-31G* energies, the αα and αγ backbones contribute a total of 59% to the Boltzmann distribution. Conformers with the γγ backbone contribute on average 15% for the HF-based geometries. The B3LYP/6-31G* optimized

Table 5. Average Bond Lengths[a] Calculated at Different Levels of Theory

level of theory	O_4-H_7	O_6-H_8	O_5-H_9	C_3-O_5	C_2-O_6	C_1-O_4	C_1-C_2	C_2-C_3	C_1-H_{10}	C_1-H_{11}	C_2-H_{12}	C_3-H_{14}	C_3-H_{13}
HF/6-31G*	0.95	0.95	0.95	1.40	1.41	1.40	1.52	1.52	1.09	1.09	1.09	1.09	1.09
G2(MP2)[b]	0.97	0.97	0.97	1.42	1.43	1.43	1.52	1.52	1.10	1.10	1.10	1.10	1.10
B3LYP/6-31G*	0.97	0.97	0.97	1.42	1.43	1.42	1.53	1.53	1.10	1.10	1.10	1.10	1.10
CBS-QB3	0.96	0.96	0.96	1.43	1.43	1.43	1.53	1.53	1.10	1.10	1.10	1.10	1.10
SM5.42/HF/6-31G*	0.95	0.95	0.95	1.41	1.41	1.41	1.52	1.52	1.08	1.08	1.09	1.08	1.08

[a] Bond lengths are in angstroms. See Figure 1 for the atomic numbering. [b] Using the MP2 geometries.

Table 6. Boltzmann Distribution (298 K) Using HF Gas-Phase Geometries[a]

conformer	HF/6-31G*	B3LYP/6-31+G**//HF/6-31G*	B3LYP/6-311+G(3df,2p)//HF/6-31G*	CCSD/6-31+G**//HF/6-31G*	CCSD(T)/6-31+G**//HF/6-31G*	G2(MP2)
95	16	14	12	15	14	12
100	10	9	9	9	11	12
109	8	11	11	8	9	7
46	8	8	9	7	7	8
101	5	6	5	6	7	7
48	4	5	5	4	4	5
7	4	7	8	5	5	5
120	5	8	9	5	5	7
45	4	4	4	4	3	3
20	3	3	2	3	2	2
54	3	2	2	2	2	2
2	3	2	3	2	2	2
116	2	2	2	5	6	2
34	2	2	2	7	7	3
64	2	2	2	2	2	3
66	2	1	2	2	1	2
53	2	1	2	2	1	2
18	2	1	1	2	1	2
43	2	3	3	2	2	3
78	2	1	1	2	2	2
86	2	2	2	4	4	1
80	2	1	2	1	1	2
1	2	2	2	1	1	2
75	1	1	1	1	1	1
35	1	1	1	0	0	1
85	1	1	1	0	0	1
88	1	1	1	0	0	1
103	1	1	1	0	0	1
			Backbone[b]			
αα	16	25	21	18	16	19
α*γ*	34	34	34	32	30	31
α*β*	14	12	14	14	16	12
ββ	2	2	2	1	1	2
βγ	18	13	15	19	20	18
γγ	15	15	14	15	17	18

[a] The numbers in this table are expressed as percentages from Δ*G* (298K) values computed at the corresponding level. [b] Obtained by summation of the contributions of the identical backbone conformations.

Boltzmann distribution agrees poorly with experiment in that there is an overemphasis of conformers **100** and **46**. However, single-point energies with more flexible sets with the B3LYP/6-31G* geometries are in excellent agreement with experiment.

With the exception of the B3LYP/6-31G* level, the *γγ* backbone, which was found, both in this study and in others,[16] to be a global minimum at many levels of theory and basis sets, is *not* the largest contributor to the Boltzmann distribution. This shows the importance of the thermal and entropic corrections for obtaining accurate, relative free energies of intramolecularly hydrogen-bonded systems. Most of the structures in the Boltzmann distribution possess two to three intramolecular hydrogen bonds. The average hydrogen-bond distance is 2.34 Å for the HF/6-31G* geometries and 2.24 Å for the B3LYP geometries, and the average hydrogen-bond angles are 110.5° and 116.9°, respectively. At higher levels of theory, much better agreement with experiment is seen.

B. Gas-Phase Microwave Spectroscopic Study. Caminati and co-workers have studied jet-cooled glycerol by microwave spectroscopy.[12b] Assuming that no conformational relaxation takes place in the adiabatic expansion and a Boltzmann distribution of the rotational levels is generated in the jet, conformation **100** has been shown to be the most stable by 0.62 kcal/mol over conformation **95**. The temperature at which these experiments were carried out was not reported but was probably less than 10 K. The relative enthalpies for most of the levels at 298 and 0 K do not correlate well with these results and suggest that the jet expansion for the microwave studies did not produce an equilibrium mixture of conformers. The lack of correlation between these experiments and the ab initio and DFT calculated energies of glycerol conformers in the gas phase has been noted by others.[17]

C. Computational Studies of the Gas-Phase Boltzmann Distribution. In a molecular dynamics force-field study on glycerol in the gas and aqueous phases,[16d,16e] the mean backbone conformational energies at 300 and 400 K were calculated. The calculations found that the αα, α*γ*, and *γγ* backbones are the most stable in the gas phase. When aqueous solvent was included for the MD simulations, intermolecular interactions (gauche effects, hydrogen bonding) stabilized the αα conformation and destabilized the *γγ* conformer as the temperature decreases. Our results are consistent with this earlier MD study, as the gas-phase Boltzmann distribution calculated by ab initio and DFT methods predicts the αα and α*γ* backbone conformers to be the most stable (Tables 6 and 7). Also, on the basis of our calculations, the *γγ* backbone conformers contribute an average of 10−15% based on the level of theory and basis set.

A more recent density functional theory study,[17b] using a more limited number (13) of glycerol conformers, has indicated that the major contributors to the Boltzmann distribution are conformers with the αα (40.5%), α*γ* (45.5%), and *γγ* (12.1%) backbones at the B3LYP/6-311+G(3df,2p)//B3LYP/6-31G* level. These previous calculations heavily favored the αα, α*γ*, and *γγ* backbones in comparison to our results. This discrepancy is most likely due to the limited number of conformations considered in the prior DFT study, thereby altering the calculated

Table 7. Boltzmann Distribution (298 K) Using B3LYP Gas-Phase Geometries[a]

conformer	B3LYP/6-31G*	B3LYP/6-31+G**//B3LYP/6-31G*	B3LYP/6-311+G(3df,2p)//B3LYP/6-31G*	CCSD/6-31+G**//B3LYP/6-31G*	CCSD(T)/6-31+G**//B3LYP/6-31G*	CBS-QB3
100	34	6	6	5	8	12
46	10	6	6	5	6	6
101	7	5	4	5	7	7
95	9	12	10	15	15	12
43	3	2	2	1	2	3
7	4	6	6	4	4	5
48	4	5	5	5	5	5
45	3	4	3	4	4	3
41	1	0	0	0	0	0
120	4	8	8	1	1	7
66	1	2	2	3	3	2
18	1	1	1	0	0	0
88	1	1	1	1	1	1
83	2	3	3	3	3	1
54	3	4	4	2	2	1
55	1	0	0	0	0	0
64	1	2	3	2	1	3
1	1	1	2	2	2	1
116	1	2	3	6	5	2
19	1	0	0	0	0	0
2	1	3	3	1	1	2
80	1	2	2	2	2	2
75	1	1	1	1	1	1
61	0	1	0	0	0	0
78	1	2	2	2	2	2
53	1	2	2	2	2	2
34	1	3	3	3	3	3
85	1	0	2	1	1	1
109	0	12	10	22	19	9
86	1	2	2	1	1	2
115	1	3	3	2	2	3
			Backbone[b]			
αα	10	27	27	28	26	21
α*γ*	31	32	29	32	34	33
α*β*	4	10	11	11	10	9
ββ	2	2	2	0	1	2
βγ	12	19	21	17	16	17
γγ	41	10	9	10	13	19

[a] The numbers in this table are expressed as percentages from ΔG (298K) values computed at the corresponding level. [b] Obtained by summation of the contributions of the identical backbone conformations.

Table 8. Comparison of Calculated Boltzmann Distributions of Glycerol with That Determined by ^{1}H NMR

	gas phase		aqueous phase					
backbone	B3LYP/6-31+G**//HF/6-31G*	G2(MP2)	SM5.42/HF/6-31G*	B3LYP/6-31+G**//SM5.42/HF/6-31G*	exptl A[a,b,f]	exptl B[a,c,f]	exptl C[d,f]	av exptl[e]
αα	25	19	18	30	18	21	20	20
α*γ*	34	31	27	28	30	28	28	29
α*β*	12	12	23	20	20	21	22	21
ββ	2	2	3	2	5	5	5	5
βγ	13	18	24	16	15	15	15	15
γγ	14	18	4	4	12	10	10	10

[a] Using the approximation that $^3J_{gauche}$ and $^3J_{trans}$ coupling constants are conformationally independent. [b] Using limit values based on previous studies by Sheppard and Turner.[38a] [c] Using limit values based on previous studies by Gutowsky, Belford, and McMahon.[38b] [d] Combination of exptl A and exptl B to obtain a ratio for $^3J_{gauche}/^3J_{trans}$ such that the function of conformer population is based on the $^3J_{gauche}/^3J_{trans}$ coupling constant ratio. [e] Averaged values from exptl A, B, and C. [f] The experimental values above are the averaged values taken from the range percentage of the compostion of glycerol in D_2O (See Table IV in ref 21).

Boltzmann distribution. Our results expand on this study to give a more complete Boltzmann distribution.

D. Solution-Phase NMR Study. A conformational study of glycerol in D_2O by ^{1}H NMR spectroscopy has been performed by Van Koningsveld.[21] In this investigation, the populations of the different conformers were determined through measurement of three-bond, $^1H-^1H$ coupling constants. The backbone conformations were calculated using different parameters for the minimum and maximum limit of $^3J_{trans}$ and $^3J_{gauche}$ as detailed in Table 8. Using the SM5.42/HF/6-31G* geometries and energies to calculate the Boltzmann distribution, the total population for each backbone conformation was determined by summation of the individual conformations with identical backbone conformations. As seen in Table 8, the calculated aqueous phase results for glycerol agree remarkably well with experiment. These results indicate that the SM5.42/HF/6-31G* theoretical level does an excellent job of dealing with nonbonded interactions in glycerol.

V. Conclusions

The 126 possible conformations of 1,2,3-propanetriol (glycerol) were studied by ab initio molecular orbital and DFT

calculations in the gas and aqueous phases using multiple levels of theory and basis sets. A partial potential energy surface for glycerol as well as an analysis of the conformational properties and hydrogen-bonding trends in both phases have been obtained. For a family of conformers, the relative energies between them decreases as the size of the basis set increases and as electron correlation is included. Consistent with previous results for other intramolecularly hydrogen-bonded systems,[6,18−20] the B3LYP/6-31G* level poorly estimates the relative energies of the conformers. With the B3LYP/6-31+G** and B3LYP/6-311+G(3df,2p) single-point energies, the relative energies between the different conformations decrease and more accurately correlate to the "correct" relative energies as predicted at the CBS-QB3 and G2(MP2) levels.

The structures of the conformers are very similar for the HF and B3LYP geometries with regard to the general orientation of dihedral angles. Furthermore, the relative energies at the G2(MP2) and CBS-QB3 levels are in excellent agreement. There is similarly excellent agreement between B3LYP/6-31+G** energies based on either HF/6-31G* or B3LYP/6-31G* geometries. *The low-energy conformations in the gas phase are similar to those in aqueous solution with a preference for certain structures in the gas phase that possess favorable backbones and hydrogen-bonding arrays. Hydrogen bonding is prominent in the gas phase, and conformations with no intramolecular hydrogen bonds are not favored in the gas phase.* However, there is *not* a gross shift in relative conformer energies on moving from the gas to aqueous phases. This suggests that for systems capable of forming intramolecular hydrogen bonds, these interactions are still present in aqueous solution, but their contribution is somewhat diminished.

Our results indicate that, for an accurate determination of relative gas-phase energies, B3LYP/6-31+G** single-point energies on a HF/6-31G* or B3LYP/6-31G* geometry should be used as a good compromise between expense and accuracy. In terms of geometrical data, B3LYP/6-31G* geometries give the best structural predictions. With regard to aqueous-phase calculations for future studies on polyhydroxylated molecules, our results on glycerol show that the SM5.42/HF/6-31G* solvation model does an excellent job with nonbonded interactions (hydrogen bonding), energetics, and geometries.

Also, our results show very good agreement with both previous experimental gas-phase studies on glycerol and expand these studies to give a more complete picture of the Boltzmann distribution. The aqueous-phase Boltzmann distribution also shows excellent agreement with experimental NMR results. This indicates that the SM5.42/HF/6-31G* theoretical level does a very good job of dealing with nonbonded interactions in water.

Our calculations so far have not included the use of specific water molecules in the first solvation shell, but the inclusion of specific water molecules on this system as well as the application of solvation models to other larger molecules are currently being investigated.

Acknowledgment. This research has been supported by the Ohio State University and the National Science Foundation (T.L.L., CHE-9875163; C.M.H., CHE-9733457). We acknowledge support from The Ohio Supercomputing Center where some of these calculations were performed. C.S.C. is a recipient of a GAANN fellowship from the U.S. Department of Education. We would also like to thank Patrick R. McCarren for technical assistance and the use of the ConforMole program. We thank Christopher J. Cramer and Donald G. Truhlar for access to the MN-GSM code at the Minnesota Supercomputing Institute.

Supporting Information Available: Cartesian coordinates for HF/6-31G*, B3LYP/6-31G*, G2(MP2), CBS-QB3, and SM5.42/HF/6-31G* structures listed in Tables 1−3; tables of geometrical parameters for conformers optimized at each level of theory; PCM and CPCM results; the 126 possible staggered conformers (unoptimized); the absolute and ZPE energies for all of the structures at all levels of theory; and Tables 1 and 2 in complete form (PDF). This material is available free of charge via the Internet at http://pubs.acs.org.

JA011785R